

# Probing chiral restoration with $\rho$ -meson melting through sum rules

**Paul M. Hohler**

E-mail: [pmhohler@comp.tamu.edu](mailto:pmhohler@comp.tamu.edu)  
Cyclotron Institute and Department of Physics and Astronomy, Texas A&M University,  
College Station, TX 77843-3366, USA

**Ralf Rapp**

E-mail: [rapp@comp.tamu.edu](mailto:rapp@comp.tamu.edu)  
Cyclotron Institute and Department of Physics and Astronomy, Texas A&M University,  
College Station, TX 77843-3366, USA

**Abstract.** We investigate whether the rho-meson melting scenario is compatible with chiral symmetry restoration utilizing a comprehensive evaluation of the QCD and Weinberg sum rules at finite temperature. As input to this analysis, in-medium vector spectral functions which describe dilepton data from ultra-relativistic heavy-ion collisions are used along with temperature dependent condensates from lattice calculations, when available, or approximated by a hadron resonance gas. The combined deployment of QCD and Weinberg sum rules turns out to be rather stringent in constructing axialvector spectral functions consistent with (partial) chiral restoration.

## 1. Introduction

In the QCD vacuum, chiral symmetry is spontaneously broken by the presence of non-zero quark condensates. Lattice-QCD calculations reveal that this symmetry becomes restored at higher temperatures as the condensates progress through a pseudo-critical region around  $T_{pc} \simeq 160$  MeV [1, 2]. A long standing problem in hadronic physics is identifying an experimental signal for this transition. Ideally, this could be achieved by simultaneously measuring the medium modifications of the spectral functions of chiral partners, *e.g.*, vector ( $\rho$ ) and axialvector ( $a_1$ ) mesons; chiral restoration is then characterized by a degeneracy of the two channel's spectral functions. The vector channel has been extensively explored through dilepton spectra in ultra-relativistic heavy-ion collisions [3, 4, 5]. Theoretical calculations from hadronic effective theory using microscopic interactions [6] are consistent with the experimental data across a wide range of collision energies. These studies reveal that the  $\rho$ -meson resonance “melts” without an appreciable mass shift as the fireball cools through the pseudo-critical region [7]. Experimental access to the axialvector channel ( $a_1 \rightarrow \pi\gamma$ ) is difficult due to its small branching and large width. Thus establishing this melting as a signal for chiral restoration remains outstanding. A theoretical determination of the axialvector spectral function is therefore needed to provide the necessary connection between the  $\rho$  melting and chiral symmetry.



The direct approach would be to calculate the axialvector spectral function from effective field theory paralleling the previous work for the  $\rho$ . However, this has proven challenging [8] and has lead some to give up the natural implementation of the mesons as local gauge bosons of the chiral symmetry [9, 10]. A recent study has been able to overcome these initial problems while maintaining a local gauging procedure in vacuum [11]; work is ongoing to extend these calculations to finite temperatures.

In this paper, based on Ref. [12], we take the more modest approach by performing a sum rule analysis to ask whether the melting scenario is compatible with chiral restoration. By using the experimentally tested in-medium  $\rho$  spectral functions and constraints from lattice data, we study whether an axialvector spectral function can be found which satisfies the sum rules. For our analysis, we use both the Weinberg sum rules (WSRs) [13, 14, 15], which are responsive to chiral symmetry restoration, and QCD sum rules (QCDSRs) [16, 17], which involve additional chirally invariant condensates, to provide “maximal” constraints on the in-medium axial-/vector spectral functions. As a by-product, we test the QCDSRs for the vector channel. Similar works have been performed, e.g., in the low-temperature limit [18, 19], for heavy-quark channels [23], or by focusing on chirally odd condensates in the vector channel only [24]. A recent study [20] parallels some of the philosophies of the current work by investigating whether finite energy WSRs can be satisfied with axial-/vector spectral functions constrained by finite energy QCDSRs [21, 22].

The results presented here build upon our earlier study [25], where we quantitatively evaluated the vacuum QCDSRs and WSRs using spectral functions that accurately describe hadronic  $\tau$ -decay data [26, 27]. There we found that the WSRs (predominately WSR-1 and -2) were particularly selective in constraining the spectral functions: by requiring that they be satisfied dictated the presence of an excited  $a_1'$  state beyond the kinematic limit of the  $\tau$ -data. Such selectivity makes the sum rules a promising tool in determining in-medium axialvector spectral functions, so new insights into the mechanism of chiral symmetry restoration can be expected.

The proceeding is organized as follows. In Sec. 2, the in-medium QCDSRs and WSRs are introduced. Section 3 describes the temperature dependence of the pertinent condensates, while in Sec. 4, the axial-/vector spectral function are specified. The quantitative sum rule analysis is presented in Sec. 5. We conclude in Sec. 6.

## 2. Finite Temperature Sum Rules

Sum rules equate dispersion integrals of spectral functions to a space-like expansion where the non-perturbative coefficients are given by low energy condensates. For our purposes, the relevant spectral functions are the isovector current-current correlator in the vector ( $V$ ) and axialvector ( $A$ ) channels,

$$\Pi_{V,A}^{\mu\nu}(q^2) = -i \int d^4x e^{iqx} \langle T \bar{J}_{V,A}^\mu(x) \bar{J}_{V,A}^\nu(0) \rangle, \quad (1)$$

where the currents, in the basis of two light flavored quarks, are given by  $\bar{J}_V^\mu = \bar{q} \vec{\tau} \gamma^\mu q$  and  $\bar{J}_A^\mu = \bar{q} \vec{\tau} \gamma^\mu \gamma_5 q$ , ( $\vec{\tau}$ : isospin Pauli matrices). Here, only the charge-neutral states (isospin  $I_3=0$ ) are considered, thus isospin indices will be dropped. In vacuum, the correlator can be decomposed as

$$\Pi_{V,A}^{\mu\nu}(q^2) = \Pi_{V,A}^T(q^2) \left( -g^{\mu\nu} + \frac{q^\mu q^\nu}{q^2} \right) + \Pi_{V,A}^L(q^2) \frac{q^\mu q^\nu}{q^2} \quad (2)$$

into the 4D-transverse and longitudinal polarizations. In the vector channel,  $\Pi_V^L(q^2)=0$ , due to vector current conservation, while the partial conservation of the axial-current involves the pion pole,

$$\text{Im} \Pi_A^L(q^2) = -\pi f_\pi^2 q^2 \delta(q^2 - m_\pi^2). \quad (3)$$

At finite temperature, Lorentz symmetry is broken such that the 4D-transverse polarization is further decomposed into 3D-transverse and -longitudinal parts. In this paper, we concentrate

on the case of vanishing 3-momentum ( $\vec{q}=0$ ) for which the 3D modes are again degenerate. We define the pertinent spectral functions as

$$\rho_{V,A} = -\frac{\text{Im}\Pi_{V,A}^T}{\pi}, \quad \rho_{\bar{A}} = \rho_A - \frac{\text{Im}\Pi_A^L}{\pi}. \quad (4)$$

For the finite temperature QCDSRs, the dispersion integral of these spectral functions constitutes the left-hand side (LHS) of the sum rule, while the right-hand side (RHS) is constructed from an operator product expansion (OPE). There is a unique sum rule for the vector and axialvector channels given by [28, 29, 30]

$$\begin{aligned} \frac{1}{M^2} \int_0^\infty ds \frac{\rho_{V,\bar{A}}(s)}{s} e^{-s/M^2} &= \frac{1}{8\pi^2} \left(1 + \frac{\alpha_s}{\pi}\right) + \frac{m_q \langle \bar{q}q \rangle}{M^4} + \frac{1}{24M^4} \langle \frac{\alpha_s}{\pi} G_{\mu\nu}^2 \rangle \\ &- \frac{\pi\alpha_s}{M^6} \frac{(56, -88)}{81} \langle \mathcal{O}_4^{V,A} \rangle + \sum_h \frac{\langle \mathcal{O}_h^{d=4, \tau=2} \rangle_T}{M^4} + \frac{\langle \mathcal{O}_h^{d=6, \tau=2} \rangle_T}{M^6} + \frac{\langle \mathcal{O}_h^{d=6, \tau=4} \rangle_T}{M^6} \dots, \end{aligned} \quad (5)$$

where the space-like  $q^2$  is traded for the Borel mass  $M^2$  by the standard Borel transform. The OPE is comprised of all operators up to dimension-6, both chirally invariant and chiral order parameters. This includes the conventional scalar operators (quark, gluon, and 4-quark condensates,  $\langle \bar{q}q \rangle$ ,  $\langle \frac{\alpha_s}{\pi} G_{\mu\nu}^2 \rangle$ , and  $\langle \mathcal{O}_4^{V,A} \rangle$ , respectively), as well as non-scalar operators induced by thermal hadrons ( $h$ ), organized by dimension ( $d$ ) and twist ( $\tau$ ).

On the other hand, the dispersion integrals of the WSRs are associated with the difference between the vector and axialvector spectral functions. As such, the corresponding OPEs are expressed only in terms of chiral order parameters, while the different WSRs correspond to different moments of the dispersion integrals. The finite temperature sum rules, first formulated in Ref. [15], read

$$\text{(WSR 1)} \quad \int_0^\infty ds \frac{\Delta\rho(s)}{s} = f_\pi^2, \quad (6)$$

$$\text{(WSR 2)} \quad \int_0^\infty ds \Delta\rho(s) = f_\pi^2 m_\pi^2 = -2m_q \langle \bar{q}q \rangle, \quad (7)$$

$$\text{(WSR 3)} \quad \int_0^\infty ds s \Delta\rho(s) = -2\pi\alpha_s \langle \mathcal{O}_4^{SB} \rangle, \quad (8)$$

where  $\Delta\rho = \rho_V - \rho_A$ . The chiral breaking 4-quark condensate can be expressed in terms of the axial-/vector ones as

$$\langle \mathcal{O}_4^{SB} \rangle = \frac{16}{9} \left( \frac{7}{18} \langle \mathcal{O}_4^V \rangle + \frac{11}{18} \langle \mathcal{O}_4^A \rangle \right). \quad (9)$$

The presence of only chiral order parameters renders the WSRs particularly sensitive to chiral restoration, whereas the channel-specific QCDSRs provide independent constraints.

### 3. In-Medium Condensates

The in-medium behavior of each condensate can be estimated from a hadron resonance gas (HRG) calculation. Here, we consider all resonances with mass  $m_h \leq 2 \text{ GeV}$  [31]. Including only the effects from single-hadron matrix elements for each operator,  $\mathcal{O}$ , leads to

$$\langle \mathcal{O} \rangle_T \simeq \langle \mathcal{O} \rangle_0 + \sum_h d_h \int \frac{d^3k}{(2\pi)^3} \frac{1}{2E_h} \langle h(\vec{k}) | \mathcal{O} | h(\vec{k}) \rangle n_h(E_h), \quad (10)$$

where  $\langle \mathcal{O} \rangle_0$  is its vacuum expectation value,  $\langle h(\vec{k}) | \mathcal{O} | h(\vec{k}) \rangle$  its hadronic matrix element,  $E_h^2 = m_h^2 + \vec{k}^2$ , and  $d_h$ ,  $m_h$ , and  $n_h$  are the hadron's spin-isospin degeneracy, mass, and thermal

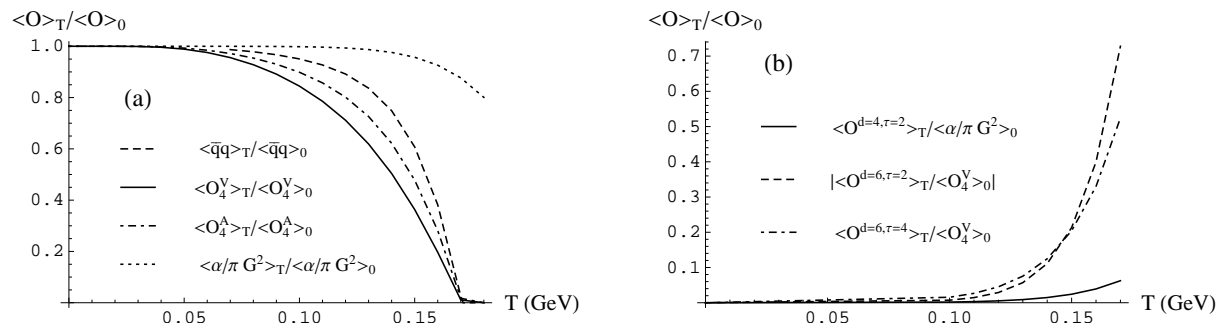


**Figure 1.** Temperature dependence of: quark, gluon, and axial-/vector 4-quark condensates relative to their vacuum values (left), and dimension-4 and dimension-6 non-scalar operators relative to the vacuum values of the gluon and vector 4-quark condensates (right).

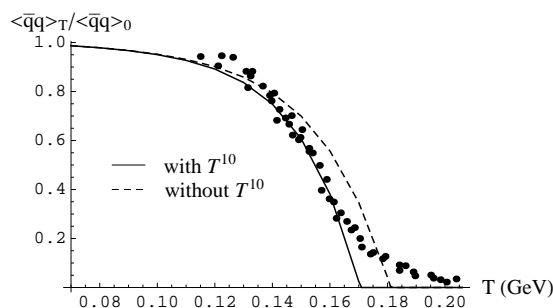


**Figure 2.** Temperature dependence of the quark condensate relative to its vacuum value, compared to thermal IQCD data [1].

distribution function (Bose ( $n_b$ ) or Fermi ( $n_f$ )), respectively. We work at zero baryon chemical potential ( $\mu_B=0$ ), so that anti-baryons can be absorbed into the degeneracy factor of baryons.

The HRG construction is known to reproduce the equation of state from IQCD quite well for  $T \leq 170$  MeV [32]. Importantly, it utilizes the same degrees of freedom as the in-medium  $\rho$  spectral function calculation. The resulting  $T$ -dependence of the quark, gluon and 4-quark condensates are depicted in Fig. 1 left, while the non-scalar operators are shown in Fig. 1 right.

The HRG correction to the quark condensate can be derived from the HRG partition function via  $\partial \ln Z / \partial m_q$  [33, 34] and has the general structure

$$\frac{\langle \bar{q}q \rangle_T}{\langle \bar{q}q \rangle_0} = 1 - \sum_h \frac{\sigma_h}{f_\pi^2 m_\pi^2} \varrho_s^h, \quad (11)$$

where  $\varrho_s^h$  is the scalar density of hadron,  $h$ , and  $\sigma_h = \langle h | \bar{q}q | h \rangle$  its  $\sigma$ -term. For the Goldstone bosons,  $\sigma_h$  can be calculated from current algebra while for all other hadrons, it is decomposed into a bare part (from the light valence quarks) [35] and a pion cloud contribution [36, 37]. Again, this decomposition parallels the medium effects of the  $\rho$  spectral function [38].

Our HRG calculation reproduces IQCD “data” [1] for  $T \lesssim 140$  MeV well, see Fig. 2. To extend this agreement, we introduced a term,  $\alpha T^{10}$ . With  $\alpha = 1.597 \cdot 10^7 \text{ GeV}^{-10}$ , the quark condensate vanishes slightly above  $T=170$  MeV. The power in  $T$  of this additional term was chosen as a balance between not affecting the low  $T$  behavior while improving the description of the high- $T$  region of the data.

For the gluon condensate, the contributions from pions and nucleons have been evaluated

in Refs. [28, 30, 39]. The HRG effect can be determined from the trace anomaly and the light quark condensate. This produces a mild dependence on temperature as shown in Fig. 1 left.

For the 4-quark condensates, current algebra again dictates the Goldstone boson contribution to the medium dependence [28]. For the non-Goldstone boson and the baryons, large  $N_c$  arguments [34, 40] suggest that their contribution can be determined by a factorization approximation which relates it to the quark condensate. We again augment the high- $T$  dependence by a term  $\beta_{V,A}T^{10}$ . Since there is no guidance from lattice data,  $\beta_{V,A}$  are adjusted for each channel to force the condensates to vanish at the same temperature as the quark condensate. This creates a dependence which is initially steeper than the quark condensate, cf. Fig. 1 left. The  $T$ -dependence of the chiral breaking 4-quark condensate follows from the axial-/vector ones via Eq. (9).

Hadrons in the heat bath also induce non-scalar condensates. For our QCDSR analysis the relevant ones are of dimension-4 twist-2,  $\langle \mathcal{O}^{d=4,\tau=2} \rangle_T$ , dimension-6 twist-2,  $\langle \mathcal{O}^{d=6,\tau=2} \rangle_T$ , and dimension-6 twist-4,  $\langle \mathcal{O}^{d=6,\tau=4} \rangle_T$ . Their  $T$  dependence, adopted from Refs. [28, 29, 30], is constructed from thermal averaged powers of the momentum, with parameters related to the light-quark parton distribution and the spin-averaged (longitudinal) structure functions for each hadron [29, 41]. For hadrons with unmeasured functions, the parameters have been approximated by using the value from either the pion or nucleon with a suppression due to the valence strange-quark content. The contributions from gluonic structure functions are believed to be numerically insignificant [28, 29] and have been neglected. To compare the relative size of these contributions, the temperature dependence, shown in Fig. 1 right, is plotted as a dimensionless ratio relative to the appropriate vacuum scalar condensate (gluon for the dimension-4 operator and the vector 4-quark for the dimension-6 operator). For the dimension-6 twist-2 operator, this ratio is negative, thus the absolute value is plotted for easier comparison.

#### 4. Finite Temperature Spectral Functions

The starting point of our study are the vacuum axial-/vector spectral functions of Ref. [12, 25]. They are constructed from three components: the ground state ( $\rho$  and  $a_1$  peaks), a first excited state ( $\rho'$  and  $a_1'$ ), and a chirally invariant (i.e., identical) continuum. The microscopic model of Ref. [42] provides the vacuum  $\rho$  spectral function, while parameterized Breit-Wigner functions are used to describe the  $a_1$ ,  $\rho'$  and  $a_1'$  resonances. The availability of experimentally measured vacuum spectral functions from  $\tau$  decays by ALEPH [26] allows the parameters of the  $a_1$  and  $\rho'$  peaks to be determined by fitting these data. The  $a_1'$  contribution, on the other hand, is deduced from the WSRs, by requiring them to be satisfied. The evaluation of the vacuum QCDSRs allows for the numerical determination of the vacuum gluon condensate and the 4-quark factorization parameter  $\kappa$  in  $\langle \mathcal{O}_4^{SB} \rangle = \frac{16}{9}\kappa \langle \bar{q}q \rangle^2$ . The resulting spectral functions are displayed in Fig. 3.

The changes of the condensates with temperature will induce modifications of the spectral functions. These modifications are accounted for as follows. Most importantly, to ensure that the results are consistent with dilepton data [7], the microscopic calculations for the  $\rho$  spectral function from hadronic effective theory [6] at vanishing baryon chemical potential are used. The only amendment we permit is a suppression of the vector-dominance coupling strength (as is commonly done in QCDSR analyses [28, 30, 43, 44]).

For the  $a_1$  meson, we parameterize the medium modifications of its spectral function by introducing four parameters (one for the mass, two for the width, and one for the axialvector-dominance coupling strength), which control the in-medium  $a_1$  peak. These parameters will be scanned at each temperature to determine whether the QCDSRs and WSRs can be satisfied.

*A priori*, the temperature dependence of the excited states is rather unconstrained. To focus the sum rules analysis on the in-medium  $a_1$  peak, we apply the model independent low-temperature effect known as chiral mixing [45, 46] to the  $\rho'$  and  $a_1'$  states instead of introducing

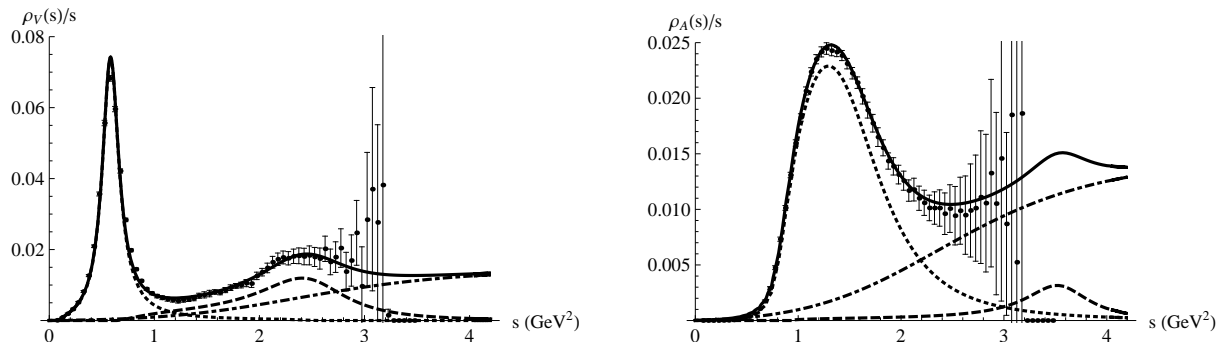


**Figure 3.** Vacuum spectral functions in the vector (left) and axialvector (right) channels, compared to experimental data for hadronic  $\tau$  decays [26]; The total spectral function in each channel (solid curve) is composed of a ground state (dotted curve), excited state (dashed curve), and a universal continuum (dot-dashed curve).

temperature dependencies to their Breit-Wigners parameters (which are hard to control). In the spirit of the HRG, both thermal pions and virtual pions from the clouds of thermal hadrons contribute to the mixing effects. Consistent with the condensates, this mixing is carried out only to linear order in the (scalar) hadron densities. In cold nuclear matter, this effect has been calculated for the pion cloud of the nucleon [47, 48]. As with the condensates, an additional  $T^{10}$  term is added to the mixing whose coefficient is determined by requiring the excited resonances become degenerate when the condensate vanishes. The addition of the virtual pions effectively approximates the extension of the mixing beyond the low- $T$  limit, yet it does not account for finite-momentum nor finite-mass corrections from the (virtual) pions.

The chirally invariant continuum is assumed to be  $T$  independent

Lastly, the  $T$  dependence of  $f_\pi(T)$  needs to be addressed. Using the Gell-Mann–Oakes–Renner relation at finite  $T$ , we relate  $f_\pi(T)$  to the already-constructed quark condensate and the pion mass, whose  $T$ -dependence is approximated by the leading-order prediction from chiral perturbation theory.

To summarize this section, a microscopic model for the  $\rho$  spectral function has been supplemented with a 4-parameter ansatz for the in-medium  $a_1$ , chiral mixing for the excited states, and a weakly  $T$ -dependent pion mass from chiral perturbation theory. This setup is now deployed to the QCDSRs and WSRs.

## 5. Finite-Temperature Sum Rule Analysis

In order to critically evaluate agreement with the sum rules, quantitative criteria are needed. For the QCDSR, we calculate the so-called  $d$ -value, *i.e.*, the average deviation between the LHS and RHS over a suitable Borel window [43, 49]. determined by using the same criteria as the vacuum analysis in Ref. [25]. From the analysis of Ref. [43], a  $d$ -value of 1% was found to encompass a reasonable uncertainty in the spectral function; we adopt this as our figure of merit.

For the WSRs, we similarly define a deviation between each side as

$$d_{\text{WSR}} = \frac{\text{LHS} - \text{RHS}}{\text{RHS}}. \quad (12)$$

The integrands of the WSRs are oscillatory functions of  $s$  with non-trivial cancelations to yield the integrated value. This can lead to “fine-tuned” solutions whereby the oscillations are still large but conspire to an apparent agreement of the sum rule, with  $\rho_V(s) \neq \rho_A(s)$  even close to restoration. To avoid an artificially fine-tuned solution, we define “absolute-value” versions of

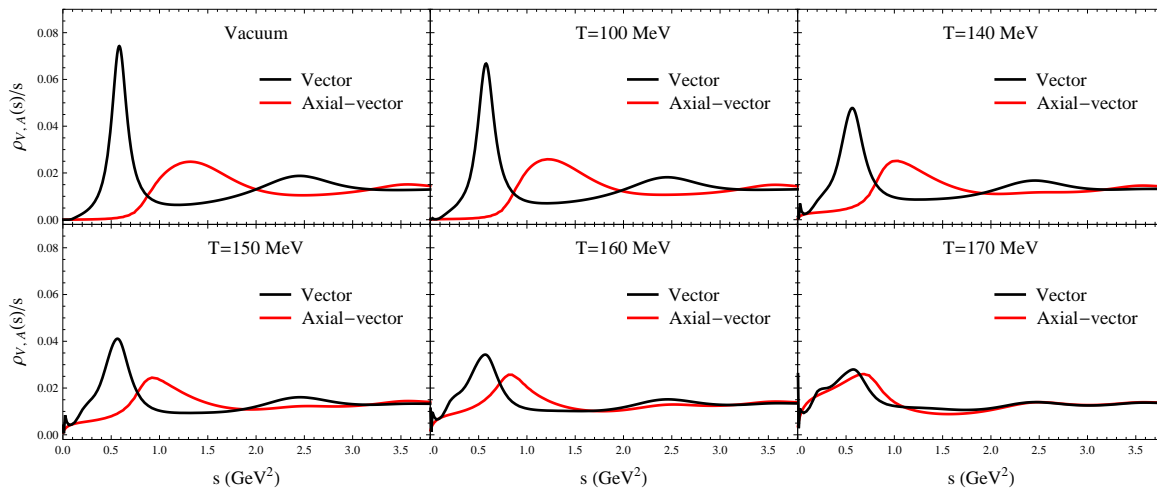


**Figure 4.** Finite-temperature vector (black curve) and axialvector (red curve) spectral functions following from minimizing Eq. (14) for the axialvector and  $d_V$  for the vector.

the LHS are defined by

$$\tilde{w}_n(T) \equiv \int_0^\infty ds s^n |\Delta\rho(s; T)|. \quad (13)$$

As the spectral functions become degenerate, these moments should decrease, even without a direct relation to chiral order parameters, and thus not allow for oscillatory cancellations. We further introduce pertinent ratios,  $r_n = \tilde{w}_n(T)/\tilde{w}_n(T=0)$ .

Our analysis proceeds as follows. First the QCDSR is evaluated for the vector channel. With a small reduction in the vector dominance coupling (up to a maximum of 7% at 170 MeV), acceptable  $d_V$  values are found for all  $T=0-170$  MeV ranging from 0.43% to 0.67%. To satisfy the axial QCDSR and the WSRs, the  $a_1$  parameters, with a smooth temperature dependence, are found by minimizing the function

$$f = d_{\text{WSR1}}^2 + d_{\text{WSR2}}^2 + d_A^2. \quad (14)$$

The resulting finite- $T$  axialvector spectral functions are shown in Fig. 4 together with the vector channel. In all cases, the deviations of WSR-1 and WSR-2 are below 0.1%, while  $d_A$  remains below 0.6%. Deviations of WSR-3 are much larger percentage-wise, but comparable to the vacuum up to  $T \simeq 150$  MeV. We find a monotonic decrease with  $T$  for each  $r_n$ -measure suggesting acceptable deviations even for WSR-3. We therefore conclude that our spectral functions are compatible with both QCDSRs and WSRs.

To gauge the uncertainty and demonstrate the selectivity of the sum rules, we present in Fig. 5 left ranges of possible axialvector spectral functions, at a fixed representative temperature  $T=150$  MeV, with certain constraints removed. The largest band, bordered by dashed curves, is the region spanned by requiring  $d_A=1\%$  for the axialvector QCDSR (the band could be larger if all spectral functions with  $d_A < 1\%$  were included). From this collection of spectral functions, we then select those which simultaneously satisfy WSR-1 better than 1% and arrive at the blue region bordered by dotted curves. This indicates that the axialvector QCDSRs alone cannot adequately distinguish possible spectral functions. Whereby, the *combination* of the QCDSR and WSRs markedly improves the selectivity of the in-medium axialvector spectral function.

An important aspect of our analysis is the systematic temperature evolution toward the restoration point at which a “trivial” degeneracy occurs, being compatible with our best

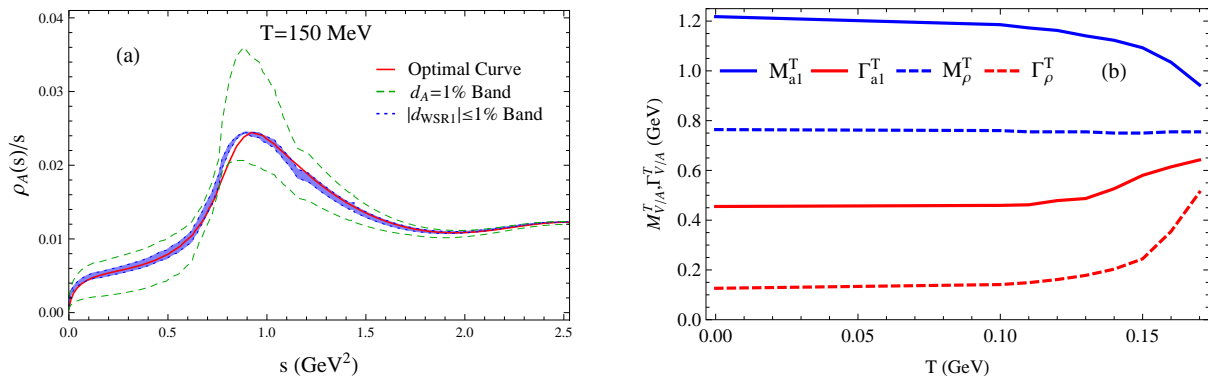


**Figure 5.** (Left panel): Allowed bands for the of axialvector spectral functions at  $T=150$  MeV when requiring agreement with the QCDSR only at  $d_A=1\%$  (dashed lines), and additionally with WSR-1 at  $|d_{WSR1}|\leq 1\%$  (dotted lines). The solid line corresponds to a minimal  $f$  value from Eq. (14). (Right panel): Temperature dependence of the  $\rho$  and  $a_1$  mass and width extracted from the spectral functions in Fig. 4.

estimates of the  $T$  dependent chiral order parameters and condensates. At  $T = 170$  MeV, the condensates have the largest deviation from lattice data, and our solutions may be more illustrative of a higher temperature where the quark condensate is closer to zero. From this evolution, we can probe the temperature dependence of  $a_1$  parameters.

We finally display in Fig. 5 right the temperature dependence of the  $\rho$  and  $a_1$  mass and width. Two fundamental characteristics of the QCD phase transition (deconfinement and chiral restoration) are exemplified here. First, the mass and width for each individual state approach each other: a sign of hadronic melting and deconfinement. Second, the two meson masses (and widths) trend towards each other (also supported by a visual inspection of Fig. 4), signaling chiral restoration. The  $\rho$ - $a_1$  merging is largely dictated by the WSRs, but the concrete shape close to chiral restoration is more sensitive to the QCDSRs. The approach toward degeneracy at finite mass implies the chiral mass splitting to “burn off”, leaving an essentially persistent “bare” masses of  $m_0 \simeq 0.8$  GeV, similar to Refs. [8, 50, 51].

## 6. Conclusions

We have investigated implications of the  $\rho$ -melting scenario as a signal of chiral restoration in hot and dense matter. To this end, we used in-medium vector spectral functions compatible with experimental dilepton data to assess whether in-medium axialvector spectral functions could be found to simultaneously satisfy the QCDSRs and WSRs. Additional input to the sum rules is the temperature dependence of pertinent condensates which was obtained from a hadron-resonance gas calculation and constrained by lattice-QCD calculations. We found agreement with the vector QCDSR with a small adjustment of the vector meson dominance coupling. Additionally, by introducing four in-medium spectral parameters for the  $a_1$ , axialvector spectral functions were deduced from a combined evaluation of QCDSR and WSRs over a temperature range from 0-170 MeV. A key feature of the resulting axialvector spectral functions is an  $a_1$  mass shift towards the  $\rho$  peak through a systematic progression in temperature toward chiral degeneracy. Furthermore, the spectral melting of both  $\rho$  and  $a_1$  resonances is suggestive for deconfinement. These insights should be subjected to further scrutiny utilizing more comprehensive microscopic calculations of the in-medium axial-/vector spectral functions. Work in this direction is on-going.

## Acknowledgments

This work is supported by the US-NSF under grant No. PHY-1306359 and by the A.-v.-Humboldt Foundation (Germany).

## References

- [1] Borsanyi S *et al.* [Wuppertal-Budapest Collaboration] 2010 *JHEP* **1009** 073
- [2] Bazavov A *et al.* 2012 *Phys. Rev. D* **85** 054503
- [3] Arnaldi R *et al.* [NA60 Collaboration] 2009 *Eur. Phys. J. C* **61** 711
- [4] Adamova D *et al.* [CERES/NA45 Collaboration] 2008 *Phys. Lett. B* **666** 425
- [5] Geurts F *et al.* [STAR Collaboration] 2013 *Nucl. Phys. A* **904-905** 217c
- [6] Rapp R and Wambach J 1999 *Eur. Phys. J. A* **6** 415
- [7] Rapp R 2013 *PoS CPOD* **2013** 008
- [8] Urban M, Buballa M and Wambach J 2002 *Phys. Rev. Lett.* **88** 042002
- [9] Urban M, Buballa M and Wambach J 2002 *Nucl. Phys. A* **697** 338
- [10] Parganlija D, Giacosa F and Rischke D H, 2010 *Phys. Rev. D* **82** 054024
- [11] Hohler P M and Rapp R 2014 *Phys. Rev. D* **89** 125013
- [12] Hohler P M and Rapp R 2014 *Phys. Lett. B* **731** 103
- [13] Weinberg S 1967 *Phys. Rev. Lett.* **18** 507
- [14] Das T, Mathur V S and Okubo S 1967 *Phys. Rev. Lett.* **19** 859
- [15] Kapusta J I and Shuryak E V 1994 *Phys. Rev. D* **49** 4694
- [16] Shifman M A, Vainshtein A I and Zakharov V I 1979 *Nucl. Phys. B* **147** 385
- [17] Shifman M A, Vainshtein A I and Zakharov V I 1979 *Nucl. Phys. B* **147** 448
- [18] Marco E, Hofmann R and Weise W 2002 *Phys. Lett. B* **530** 88
- [19] Holt N P M, Hohler P M and Rapp R 2013 *Phys. Rev. D* **87** 076010
- [20] Ayala A, Dominguez C A, Loewe M and Zhang Y *Preprint arXiv:1405.2228*
- [21] Dominguez C A, Loewe M and Zhang Y 2012 *Phys. Rev. D* **86** 034030
- [22] Ayala A, Dominguez C A, Loewe M and Zhang Y 2012 *Phys. Rev. D* **86** 114036
- [23] Hilger T, Kampf B and Leupold S 2011 *Phys. Rev. C* **84** 045202
- [24] Hilger T, Thomas R, Kampf B and Leupold S 2012 *Phys. Lett. B* **709** 200
- [25] Hohler P M and Rapp R 2012 *Nucl. Phys. A* **892** 58
- [26] Barate R *et al.* [ALEPH Collaboration] 1998 *Eur. Phys. J. C* **4** 409
- [27] Ackerstaff K *et al.* [OPAL Collaboration] 1999 *Eur. Phys. J. C* **7** 571
- [28] Hatsuda T, Koike Y and Lee S H 1993 *Nucl. Phys. B* **394** 221
- [29] Leupold S and Mosel U 1998 *Phys. Rev. C* **58** 2939
- [30] Zschocke S, Pavlenko O P and Kämpfer B 2002 *Eur. Phys. J. A* **15** 529
- [31] Nakamura K *et al.* (Particle Data Group) 2010 *J. Phys. G* **37** 075021
- [32] Karsch F, Redlich K and Tawfik A 2003 *Eur. Phys. J. C* **29** 549
- [33] Gerber P and Leutwyler H 1989 *Nucl. Phys. B* **321** 387
- [34] Leupold S 2006 *J. Phys. G* **32** 2199
- [35] Gasser J, Leutwyler H and Sainio M E 1991 *Phys. Lett. B* **253** 252
- [36] Jameson I, Thomas A W and Chanfray G 1992 *J. Phys. G* **18** L159
- [37] Birse M C and McGovern J A 1992 *Phys. Lett. B* **292** 242
- [38] Rapp R 2013 *J. Phys. Conf. Ser.* **420** 012017
- [39] Cohen T D, Furnstahl R J and Griegel D K 1992 *Phys. Rev. C* **45** 1881
- [40] Leupold S 2005 *Phys. Lett. B* **616** 203
- [41] Choi S, Hatsuda T, Koike Y and Lee S H 1993 *Phys. Lett. B* **312** 351
- [42] Urban M, Buballa M, Rapp R and Wambach J 1998 *Nucl. Phys. A* **641** 433
- [43] Leupold S, Peters W and Mosel U 1998 *Nucl. Phys. A* **628** 311
- [44] Leupold S 2001 *Phys. Rev. C* **64** 015202
- [45] Dey M, Eletsky V L and Ioffe B L 1990 *Phys. Lett. B* **252** 620
- [46] Steele J V, Yamagishi H and Zahed I 1996 *Phys. Lett. B* **384** 255
- [47] Chanfray G, Delorme J and Ericson M 1998 *Nucl. Phys. A* **637** 421
- [48] Krippa B 1998 *Phys. Lett. B* **427** 13
- [49] Leinweber D B 1997 *Ann. Phys.* **254** 328
- [50] Pisarski R D *Preprint hep-ph/9503330*
- [51] Pisarski R D 1995 *Phys. Rev. D* **52** 3773